Noname manuscript No.
(will be inserted by the editor)

Igor V. Andrianov · Vladyslav V. Danishevskyy · Heiko Topol · Graham A. Rogerson

Propagation of Floquet-Bloch shear waves in viscoelastic composites: analysis and comparison of interface/interphase models for imperfect bonding

Received: date / Accepted: date

Abstract The phononic band structure of waves, which travel though composites, result from the geometric and mechanical properties of the materials and from the interaction of the different constituents. In this article, we study two different models to simulate imperfect bonding and their impact on the phononic bands: (a) imperfect bonding is simulated by introducing an artificial interphase constituents with properties which define the bonding quality; (b) imperfect bonding is described by conjugate conditions in the interface, in which the difference in the displacement is proportional to the interfacial stress. Viscoelastic behavior of the constituents has a crucial influence on the traveling signal, and the wave attenuates with increasing viscosity. We study the interaction of the different bonding conditions and the viscoelastic behavior as well as the impact of such interplay on the wave attenuation and dispersion characteristics of the material.

Keywords wave propagation · imperfect bonding · viscoelasticity

1 Introduction

Thin coatings around inclusions are used in different applications of composites, for example as a mean to compensate the poor adhesion between fibers and the constituent matrix, and to increase the ability to carry higher loads [43]. Karpinos & Fedorenko [25] discuss the advantage of the mechanical properties of composites with coatings between fibers and the matrix over composites with uncoated fibers after high temperature production.

Imperfect bonding between components plays a crucial role in the functionality and reliability of composites, and it might result from the lack of adhesion between the constituent and cracks. Imperfect bonding might also result from corrosion, as discussed in the work of Germain & Pamin [16]. In mechanical modeling, there exist different approaches to describe such imperfect conditions. One example is the so-called spring layer model, in which the differences in the displacements at the common interface of two constituents are proportional to the stress in the interface. Works which

Igor V. Andrianov
Institute of General Mechanics, RWTH Aachen University, Templergraben 64, 52062 Aachen, Germany
E-mail: igor_andrianov@hotmail.com

Vladyslav V. Danishevskyy
School of Computing and Mathematics, Keele University, Staffordshire, ST5 5BG, UK
E-mail: v.danishevskyy@keele.ac.uk

Heiko Topol
Center for Advanced Materials, Qatar University, P.O. Box 2713, Doha-Qatar
E-mail: htopol@qu.edu.qa

Graham A. Rogerson
School of Computing and Mathematics, Keele University, Staffordshire, ST5 5BG, UK
E-mail: g.rogerson@keele.ac.uk

employ this approach are, for example, Geymonat et al. [17], Klarbring [26], and Krasucki & Lenci [27]. Another way to model imperfect bonding is to introduce an artificial interphase of small thickness between the constituents, with the properties of the interphase describing the quality of the bonding [19, 21].

A challenging goal in the different fields of mechanics, is to identify the internal structure of a heterogeneous material by measurement of its macroscopic properties. This approach has great importance for various practical applications, such as non-destructive testing of composites, non-invasive diagnostic of biological tissues (e.g., bones, cartilages), detecting the texture of soils and rocks for the purposes of geological explorations, and many others. One solution to this problem is the investigation of wave propagation in periodic media. A heterogeneous solid possesses a complicated pattern of frequency bands which consist of so-called pass bands, for which wave propagation is possible, and stop bands, for which traveling waves attenuate. In analogy to the photonic bands for electromagnetic waves, the frequency bands for propagating waves in solids are also denoted as phononic bands. If the frequency of the signal falls into a stop band, a stationary wave is excited and neighboring heterogeneities (e.g., particles) vibrate in alternate directions. On the macro level, the amplitude of the global wave attenuates exponentially so that wave propagation is not possible. Thus, a composite can play the role of a wave filter. This effect of wave propagation and attenuation described above has great practical importance. Theoretical prediction of the phononic band structures may help to design new composites for a large variety of engineering applications, such as vibrationless environments for high-precision mechanical systems, acoustic filters, noise control devices, ultrasonic transducers, etc.

Phononic bands can be predicted theoretically by the Floquet-Bloch approach [8, 14]. This approach has been documented in the book by Brillouin [9], and it has been utilized by many authors [3, 40]. The basic idea is to represent the unknown solution as an effective wave modulated by some spatially periodic functions; such a modulation aims to describe the influence of the composite microstructure. The problem essentially reduces to a spectral eigenvalue problem that allows us to evaluate the dispersion curves and thus to determine pass and stop bands of the material.

In the case of one-dimensional problems, e.g., for layered composites, it is usually possible to derive the exact dispersion equations [7, 40]. In the case two-dimensional and three-dimensional problems, unknown fields as well as the material properties in a heterogeneous medium can be expressed by some infinite series expansions. Examples are the plane-wave expansions method [28], the Rayleigh multipole-expansions method [36], and the Korringa-Kohn-Rostoker method (also known as the multiple scattering method [39]). All of these methods represent the solution by some infinite series expansions and their convergence usually depends on the contrast between the properties of the components. Another widely used approach to study wave propagation in periodic media is the finite difference time domain method (see, for instance, the paper [35] and cited references therein).

One of the first papers to discuss wave propagation in composites and the resulting frequency band structure was written by Lee & Yang [30]. Properties of Floquet-Bloch waves were interpreted in terms of the normal mode theory, and the high frequency limit for Floquet-Bloch waves is investigated and interpreted in terms of geometrical optics type analysis. The bulk of research in this field is devoted to elastic case, and the articles of Guz & Shul'ga [20], Shul'ga [42], and Mead [34] review the different achievements in this field. They analyzed a banded structure of the frequency spectrum composed of pass and stop bands. Properties of Floquet-Bloch waves were interpreted in terms of the normal mode theory and the high frequency limit for Floquet-Bloch waves is investigated and interpreted in terms of geometrical optics type analysis. Studies of the 1D [11] and 2D periodical lattices [12, 34] provide a better understanding of the behavior of real composites.

Wave propagation in damped and viscoelastic media has been also treated by many authors. Mace & Manconi [33] analyzed the influence of damping on dispersion curves for strings and beams without and with elastic foundations. The general dispersion and dissipation relations for a 1D viscoelastic lattice were obtained by Wang et al. [45]. Liu et al. [31] studied wave propagation in 2D viscoelastic Kelvin-Voigt type phononic crystals using a finite difference time domain method. The article of Merheb et al. [35] is devoted to the transmission of acoustic waves through elastic and viscoelastic Maxwell-Wiechert type 2D silicone rubber/air phononic crystal structures. Their calculations were based on a finite difference time domain method. The works of Guz & Shulga [20] and Shulga [42] were based on the concepts of complex moduli and the Floquet-Bloch approach. Hussein [23] gives a detailed analysis of the effects of damping on the frequency band structure and associated phase and group velocity dispersion curves for periodical composite material. Ideal contact between the constituents is

supposed. Linear and isotropic elastic response and Rayleigh-type damping are assumed. The articles of Nouh et al. [38] and Wang et al. [46] investigate wave propagation in metameterials with periodic microstructure and viscoelastic constitutes.

Our paper has the focus on the investigation of the interaction of viscoelastic behavior and imperfect bonding, and it is organized as follows: Section 2 investigates one-dimensional shear wave propagation in layered elastic composites for imperfect bonding. To simulate imperfect bonding, two approaches are taken into our consideration. In the first part, bonding is simulated by a thin interphase material. The thickness is taken to be much smaller than the dimensions of other constituents. The properties of this interphase defines the bonding conditions. The second approach defines the bonding conditions to the spring-layer model, in which the difference in displacement is assumed proportional to the governing shear stresses in the interface. These approaches are compared numerically. In Section 3, we investigate the interaction of viscoelastic behavior and imperfect bonding. The results are obtained by application of the Floquet-Bloch approach, which provides exact results for the dispersion relations. In Section 4, we apply the plane-wave expansion method to obtain the relation between the wave number and the frequency of the propagating wave. In the first part, the results from the plane-wave expansion method are compared to the results of the exact solution. In the second part, a brief example is provided, in which shear wave propagation in a fibrous composite with periodic microstructure is analyzed. The final sections discuss the results and provide some concluding remarks.

2 One-dimensional wave propagation in layered elastic composites

In this section, we consider shear wave propagation through a spatially infinite layered composite with imperfect bonding between the constituents. To analyze the dispersion relation of the composite in the form of frequency bands, e.g., pass bands where wave propagation is possible, and stop bands where the traveling signal attenuated exponentially, we apply the Floquet-Bloch approach, which is based on the works of Floquet [14] and Bloch [8]. Note that in the literature this approach is also called the Floquet-Lyapunov theorem or Bloch theorem. Floquet himself proved it for the function of one variable satisfying the well-known Mathieu equation [14]. Lyapunov generalized this to a vector function of one variable [32], and later Bloch to functions of several variables [8]. This theory is a direct consequence of the translation symmetry of a structure, and it allows us to obtain an exact solution for the pass and stop band structures for relatively simple problems such as the herein considered layered composite. Despite the limitation of this approach to simple geometries, the exact solutions to such simple problems present a useful reference for solutions, which have been obtained numerically, for example by the plane-wave expansion method, which will be treated in Sec. 4.

The composite structure is periodically repeating and possessing layers of finite thickness in x-direction. The wave equation for a shear wave propagation in x-direction at time t has the form

$$\frac{\partial}{\partial x}\left[G(x)\frac{\partial w(x,t)}{\partial x}\right] = \rho(x)\frac{\partial^2 w(x,t)}{\partial t^2}, \tag{1}$$

where $G(x)$ is the shear modulus, $\rho(x)$ is the mass density, and $w(x,t)$ is the transverse displacement at location x. The coefficients in Eq. (1) are discontinuous functions, so that the solution of (1) must be treated in a weak sense [29]. The material properties of the components are considered to be constant in the individual constituents $\Omega^{(a)}$, $a = 1, 2, \ldots$, and the displacements to be continuous function of both x and t,

$$G(x) = G^{(a)}, \quad \rho(x) = \rho^{(a)}, \quad w(x,t) = w^{(a)}(x,t), \quad x \in \Omega^{(a)}. \tag{2}$$

Applying (2), the wave Eq. (1) for the individual constituents $\Omega^{(a)}$ can be rewritten as

$$G^{(a)}\frac{\partial^2 w^{(a)}}{\partial x^2} = \rho^{(a)}\frac{\partial^2 w^{(a)}}{\partial t^2} \quad \text{in} \quad \Omega^{(a)}. \tag{3}$$

It remains on open problem, that a solution to the partial differential Eq. (3) can just be presented in a general form. In order to obtain a solution, which is unique, additional boundary conditions or initial conditions have to be introduced. The herein applied Floquet-Bloch approach gives a general solution to a harmonic wave with unknown coefficients, which, in order to determine the dispersion relation, do not have to be determined explicitly.

The dispersion relation results from the properties of the constituents and from the quality of the bonding between the different constituents. Imperfect bonding between the constituents is taken into our considerations by two different approaches:

- In the first case, imperfect bonding is simulated by an *artificial interphase* of thickness considered small in comparison to the dimensions of the other constituents. The length and the material properties of this interphase define the bonding behavior. This case will be discussed in detail in Sect. 2.1.
- In the second case, bonding between the constituents is directly described by the conjugate conditions at the common *interface*, by application of the spring-layer model. This case will be discussed in detail in Sect. 2.2.

In Sect. 2.3, the solutions of both approaches are compared. Such methodology allows us to develop models for composites with imperfect bonding, in which other than perfect bonding conditions are not taken explicitly into account, for example by the application of the plane-wave expansion method, which will be discussed in detail in Sect. 4.

2.1 Imperfect bonding simulated by an interphase constituent

One periodically repeated unit cell of the layered structure consists of the inclusion $\Omega^{(1)}$, the matrix $\Omega^{(3)}$, and the interphase $\Omega^{(2)}$ between the components $\Omega^{(1)}$ and $\Omega^{(3)}$. The thicknesses of the different layers are illustrated in Fig. 1. This interphase $\Omega^{(2)}$ is considered to be thin in comparison to the

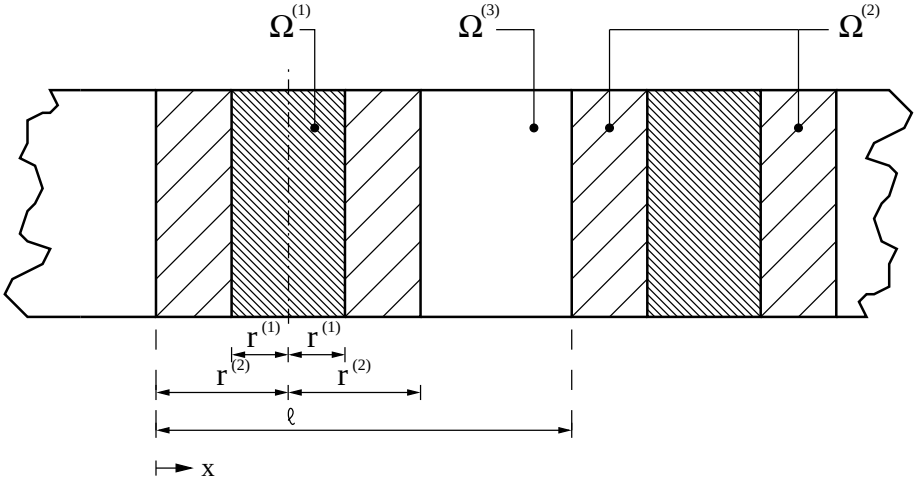

Fig. 1 A layered composite, which consists of periodical structure of the inclusion $\Omega^{(1)}$, the matrix $\Omega^{(3)}$, and the interphase $\Omega^{(2)}$.

lengths ℓ of the unit cell and the thickness $2r^{(1)}$ of the constituent $\Omega^{(1)}$,

$$\frac{r^{(2)} - r^{(1)}}{\ell} \ll 1. \tag{4}$$

Bonding between all neighboring constituents is taken to be perfect, so that both the shear stresses and the displacements of two constitutes $\Omega^{(i)}$ and $\Omega^{(i+1)}$ are considered to be equal at their common interface $\partial\Omega_{i,i+1}$, thus

$$\left\{ G^{(i)} \frac{\partial w^{(i)}}{\partial x} = G^{(i+1)} \frac{\partial w^{(i+1)}}{\partial x} \right\}\Big|_{\partial\Omega_{i,i+1}}, \tag{5a}$$

$$\left\{ w^{(i)} = w^{(i+1)} \right\}\Big|_{\partial\Omega_{i,i+1}}, \tag{5b}$$

where $i = 1, 2$.

This problem is now analyzed within a single unit cell of the length ℓ. Therefore, we consider a harmonic wave in the form

$$w^{(i)}(x,t) = F^{(i)}(x) \exp\left[j(\mu x + \omega t)\right] \quad \text{in } \Omega^{(i)}, \quad i = 1, 2, 3, \tag{6}$$

where μ is the wave number, ω is the frequency, $j = \sqrt{-1}$, and

$$F^{(i)}(x) = F^{(i)}(x + p\ell) \tag{7}$$

are spatially periodic functions which describe the influence of the microstructure. The factor of ℓ in (7) is an integer, $p = \pm 1, \pm 2, \ldots$. From (6) and (7) one can conclude that that the displacement $w^{(i)}(x,t)$ at a location x and the displacement $w^{(i)}(x + \ell, t)$ at a location $x + \ell$ are related via

$$w^{(i)}(x + \ell, t) = w^{(i)}(x,t) \exp\left(j\mu\ell\right). \tag{8}$$

The frequency band structure of the composite can be determined by rewriting the wave number μ in complex notation as

$$\mu = \mu_R + j\mu_I, \tag{9}$$

where μ_R is the real part and μ_I is the imaginary part of the wave number. The ω vs. μ_R diagram represents the pass bands, for which wave propagation is possible, and the ω vs. μ_I diagram represents the stop bands, for which the traveling signal attenuates exponentially. After substitution of ansatz (6) into the wave Eq. (3) for the individual constituents, we derive the function (7) in the form

$$F^{(i)}(x) = F_1^{(i)} \left[j\left(\mu^{(i)} - \mu\right) x\right] + F_2^{(i)} \exp\left[-j\left(\mu^{(i)} + \mu\right) x\right], \tag{10}$$

where $F_1^{(i)}$ and $F_2^{(i)}$ are constant coefficients and $\mu^{(i)} = \omega\sqrt{\rho^{(i)}/G^{(i)}}$ is the wave number of the component $\Omega^{(i)}$.

Within the unit cell $0 \le x \le \ell$, the boundary conditions (5a) and (5b) become:

$$\left\{ G^{(1)} \frac{\partial w^{(1)}}{\partial x} = G^{(2)} \frac{\partial w_-^{(2)}}{\partial x} \right\}\Bigg|_{x = r^{(2)} - r^{(1)}}, \tag{11a}$$

$$\left\{ w^{(1)} = w_-^{(2)} \right\}\Big|_{x = r^{(2)} - r^{(1)}}, \tag{11b}$$

$$\left\{ G^{(1)} \frac{\partial w^{(1)}}{\partial x} = G^{(2)} \frac{\partial w_+^{(2)}}{\partial x} \right\}\Bigg|_{x = r^{(1)} + r^{(2)}}, \tag{11c}$$

$$\left\{ w^{(1)} = w_+^{(2)} \right\}\Big|_{x = r^{(1)} + r^{(2)}}, \tag{11d}$$

$$\left\{ G^{(3)} \frac{\partial w^{(3)}}{\partial x} = G^{(2)} \frac{\partial w_+^{(2)}}{\partial x} \right\}\Bigg|_{x = 2r^{(2)}}, \tag{11e}$$

$$\left\{ w^{(3)} = w_+^{(2)} \right\}\Big|_{x = 2r^{(2)}}, \tag{11f}$$

where the subscript " $-$ " indicates the interphase on the left side of the inclusion $\Omega^{(1)}$, and the subscript "$+$" indicates the interphase on the right side of the inclusion. Taking into consideration the periodicity condition (7), the outer boundaries of the unit cell are coupled by the following conditions:

$$\left\{ G^{(3)} \frac{\partial w^{(3)}}{\partial x} \right\}\Big|_{x=\ell} - \left\{ G^{(2)} \frac{\partial w_-^{(2)}}{\partial x} \right\}\Big|_{x=0} \exp\left(j\mu\ell\right) = 0, \tag{12a}$$

$$\left\{ w^{(3)} \right\}\Big|_{x=\ell} - \left\{ w_-^{(2)} \right\}\Big|_{x=0} \exp\left(j\mu\ell\right) = 0. \tag{12b}$$

Equation (12a) couples the stresses at the outer boundaries, and (12b) couples the displacements.

In Eqs. (11) and (12) we find a system of eight linear algebraic equations in the eight unknown coefficients $F_i^{(1)}$, $F_{i-}^{(2)}$, $F_{i+}^{(2)}$, and $F_i^{(3)}$, $i = 1, 2$. If the determinant of the matrix of coefficients is set equal to zero, the system has a nontrivial solution which gives an exact relation between ω and μ, the dispersion relation. Exact dispersion relations for linear elastic layered composites with perfect bonding between the components are well known. For example, Shen & Cao [41] provide a solution for an arbitrary number of layers.

2.2 Imperfect bonding described by conjugate conditions

In the present section, we analyze wave propagation through a composite which consists of a matrix $\Omega^{(3)}$ and inclusions $\Omega^{(1)}$. A single unit cell of the layered structure is shown in Fig. 2. We want to directly

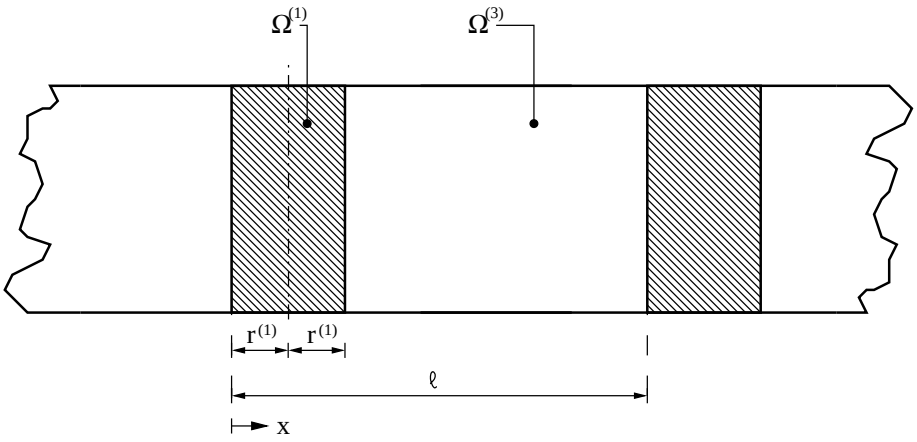

Fig. 2 One unit cell of the periodically repeated structure consisting of the inclusion material $\Omega^{(1)}$, and the matrix material $\Omega^{(3)}$. Here the bonding at $\partial\Omega_{1,3}$ is considered to be imperfect.

apply conjugate conditions, which describe the quality of the bonding between $\Omega^{(1)}$ and $\Omega^{(3)}$. Therefore, we apply the spring-layer model. Let us explain this model in detail. Usually, stresses are continuous across the interface, while the displacements may be continuous or discontinuous. In the spring-layer model it is assumed that the interfacial stress is a function of the difference in the displacements. This model was initially proposed by Goland and Reissner [19]. The asymptotic justification of the spring-layer model was proposed by different authors [17, 26, 27]. These works derived the spring-layer model asymptotically, assuming that the interface is a layer with a thickness which tends to zero. While the present article restricts the mechanical properties to linear behavior, we want to refer to the articles of Danishevs'kyy et al. [13] to provide an example for nonlinear interface conditions, and to the article of Andrianov et al. [6], in which material behavior, as well as the interface conditions, are taken to be nonlinear.

In Sect. 2.1 we simulated imperfect bonding by an artificial interphase, while in the present section we apply the spring-layer model. By contrasting these results, we can estimate the properties of the artificial interphase to simulate certain interfacial mechanical properties.

To derive the spring-layer model, let us consider the interphase $\Omega^{(2)}$ with the thickness $\Delta r = r^{(2)} - r^{(1)}$ and the shear modulus $G^{(2)}$ between the inclusion $\Omega^{(1)}$ and the matrix $\Omega^{(3)}$ in Fig. 3. At the interface $\partial\Omega_{1,2}$ between the inclusion $\Omega^{(1)}$ and the interphase $\Omega^{(2)}$ and at the interface $\partial\Omega_{2,3}$ between

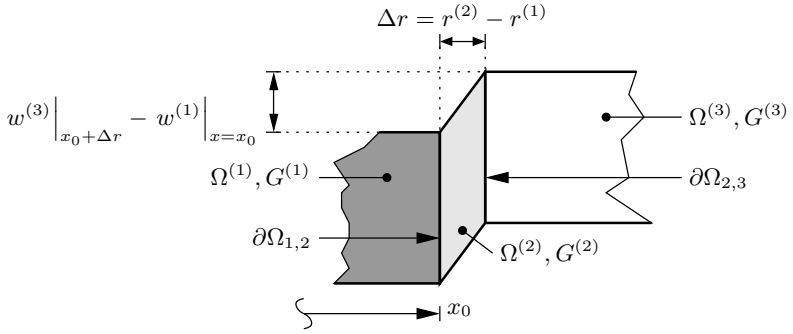

Fig. 3 Imperfect bonding between an inclusion material $\Omega^{(1)}$ and the matrix material $\Omega^{(3)}$ simulated by the layer $\Omega^{(2)}$ with the thickness $\Delta r = r^{(2)} - r^{(1)}$ and the shear modulus $G^{(2)}$.

the interphase $\Omega^{(2)}$ and the matrix $\Omega^{(3)}$ we assume perfect bonding between the constituents,

$$\left\{w^{(1)} = w^{(2)}\right\}\Big|_{\partial\Omega_{1,2}}, \tag{13a}$$

$$\left\{\tau^{(1)} = \tau^{(2)}\right\}\Big|_{\partial\Omega_{1,2}}, \tag{13b}$$

$$\left\{w^{(2)} = w^{(3)}\right\}\Big|_{\partial\Omega_{2,3}}, \tag{13c}$$

$$\left\{\tau^{(2)} = \tau^{(3)}\right\}\Big|_{\partial\Omega_{2,3}}, \tag{13d}$$

where $\tau^{(a)} = G^{(a)}\frac{\partial w^{(a)}}{\partial x}$ are the shear stresses in the constituents $\Omega^{(a)}$, $a = 1, 2, 3$. For a thin ($\Delta r \to 0$) interphase $\Omega^{(2)}$ we can take the assumption

$$\left|\frac{\partial w^{(2)}}{\partial x}\right| \gg \left|\frac{\partial w^{(2)}}{\partial t}\right|, \tag{14}$$

so that wave Eq. (3) for $\Omega^{(2)}$ becomes

$$G^{(2)}\frac{\partial^2 w^{(2)}}{\partial x^2} \approx 0. \tag{15}$$

Equation (15) has the solution

$$w^{(2)} = C_1 x + C_2, \tag{16}$$

where C_1 and C_2 and two integration constants, which can be determined from boundary conditions (13a) and (13c) as follows:

$$C_1 = \frac{1}{\Delta r}\left(w^{(3)}\Big|_{\partial\Omega_{1,2}} - w^{(1)}\Big|_{\partial\Omega_{2,3}}\right), \tag{17a}$$

$$C_2 = w^{(1)}\Big|_{\partial\Omega_{2,3}} - \frac{x_0}{\Delta r}\left(w^{(3)}\Big|_{\partial\Omega_{1,2}} - w^{(1)}\Big|_{\partial\Omega_{2,3}}\right). \tag{17b}$$

From either (13b) or (13d), which demand equal shear stresses at the interfaces $\partial\Omega_{1,2}$ and $\partial\Omega_{2,3}$, the difference between the displacements $w^{(3)}$ and $w^{(1)}$ at the boundaries to $\Omega^{(2)}$ then become

$$w^{(3)}\Big|_{\partial\Omega_{1,2}} - w^{(1)}\Big|_{\partial\Omega_{2,3}} = \tau^{(2)}\frac{\Delta r}{G^{(2)}}. \tag{18}$$

To quantify the quality of the bonding between the constituents $\Omega^{(1)}$ and $\Omega^{(3)}$ at their interface $\partial\Omega_{13}$, we introduce the bonding factor γ in the form

$$\gamma = \lim_{\substack{G^{(2)}\to 0 \\ \Delta r\to 0}} \frac{\Delta r}{G^{(2)}} = \text{const.} \tag{19}$$

If $\gamma = 0$, then the bonding is perfect. With increasing values for γ the bonding quality decreases. In the limiting case $\gamma \to \infty$, there is no bonding between the constituents.

If we take the stress distribution to be homogeneous in the interface, we arrive at the following condition for the difference of the displacements at the boundary $\partial\Omega_{1,3}$ between the inclusion and the matrix:

$$\left\{ \pm \left(w^{(3)} - w^{(1)} \right) = \gamma G^{(1)} \frac{\partial w^{(1)}}{\partial x} \right\}\Bigg|_{\partial\Omega_{1,3}} . \tag{20}$$

The upper algebraic sign in $\pm$ belongs to the boundary on the right side of $\Omega^{(1)}$, and the lower sign to the left side. This bonding model is discussed in detail by Andrianov et al. [6]. The stresses in the interface $\partial\Omega_{1,3}$ between the matrix and the inclusion are assumed to be equal, and independent from the stipulation of the bonding factor γ, thus

$$\left\{ G^{(1)} \frac{\partial w^{(1)}}{\partial x} = G^{(3)} \frac{\partial w^{(3)}}{\partial x} \right\}\Bigg|_{\partial\Omega_{1,3}} . \tag{21}$$

The governing situation will be analyzed within the unit cell $0 \le x \le \ell$. The propagating wave is again described by the ansatz presentation in Eq. (6), which, after substitution into the wave Eq. (3) for the individual constituents results into (10) with the four coefficients $F_i^{(1)}$ and $F_i^{(3)}$, $i = 1, 2$.

Within this unit cell, the boundary conditions in (20) and (21) become

$$\left\{ G^{(1)} \frac{\partial w^{(1)}}{\partial x} = G^{(3)} \frac{\partial w^{(3)}}{\partial x} \right\}\Bigg|_{x=2r^{(1)}} , \tag{22a}$$

$$\left\{ w^{(3)} - w^{(1)} = \gamma G^{(1)} \frac{\partial w^{(1)}}{\partial x} \right\}\Bigg|_{x=2r^{(1)}} . \tag{22b}$$

Recalling condition (8), which results from the periodicity of the composite, the outer boundaries $x = 0$ and $x = \ell$ of the unit cell are coupled via

$$\left\{ G^{(3)} \frac{\partial w^{(3)}}{\partial x} \right\}\Bigg|_{x=\ell} = \left\{ G^{(1)} \frac{\partial w^{(1)}}{\partial x} \right\}\Bigg|_{x=0} \exp\left(j\mu\ell\right), \tag{23a}$$

$$-\left\{ w^{(3)} \right\}\Big|_{x=\ell} + \left\{ w^{(1)} \right\}\Big|_{x=0} \exp\left(j\mu\ell\right) = \left\{ \gamma G^{(1)} \frac{\partial w^{(1)}}{\partial x} \right\}\Bigg|_{x=0} \exp\left(j\mu\ell\right). \tag{23b}$$

In (22) and (23) we find a system of four equations. If the determinant of the matrix of the coefficients $F_i^{(1)}$, $F_i^{(3)}$, $i = 1, 2$ is set equal to zero, then we obtain from the condition for existence of a non-trivial solution the dispersion relation, which allows us to determine the stop bands and pass bands of the material. The solution is presented in Appendix A.

2.3 Numerical examples

The numerical example section consists of two parts. The first part shall illustrate the influence of the bonding factor γ on the dispersion relation. The second contrasts the solutions for the frequency band structure when the bonding condition is simulated by an artificial interphase between the inclusion and the matrix, as discussed in Sect. 2.1, and when the bonding condition is described by the conjugate conditions at the interface between the constituents, as discussed in Sect. 2.2.

Dispersion relation for imperfect bonding: We consider a composite as shown in Fig. 2, with the unit cell length ℓ, and $r^{(1)}/\ell = 0.1$. This composite is composed of a polyethylene matrix ($G^{(3)} = 0.117$ GPa, $\rho^{(3)} = 910$ kg/m^3) and steel inclusions ($G^{(1)} = 80$ GPa, $\rho^{(1)} = 7860$ kg/m^3). The material parameters are taken from [10]. The frequency band structure is obtained from Eqs. (22) and (23). The wave number is separated into a real part and an imaginary part, as given by (9). The results are illustrated in Fig. 4 for different values of the bonding factor γ, where the normalizations $\bar{\mu} = \mu\ell$ and $\bar{\omega} = \omega\ell$ are applied. Due to such normalization, $\bar{\mu}$ becomes dimensionless, and its real part takes values in the

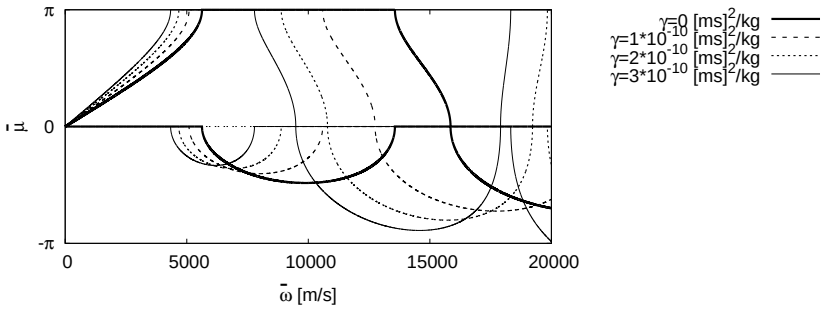

Fig. 4 Frequency band structure of a layered polyethylene ($G^{(3)} = 0.117$ GPa, $\rho^{(3)} = 910$ kg/m^3) and steel ($G^{(1)} = 80$ GPa, $\rho^{(1)} = 7860$ kg/m^3) composite for different values of γ, where the normalizations $\bar{\mu} = \mu\ell$ and $\bar{\omega} = \omega\ell$ are applied. The pass bands ($\mu_R \neq 0, \mu_I = 0$) are plotted as positive values, and the stop bands ($\mu_R = 0, \mu_I \neq 0$) are plotted as negative values.

range between zero and π. This diagram shows that with increasing values for γ, the frequency bands shift closer together, and the local extrema of the attenuation factors change their values. For this example, the extremum of the first stop band decreases, while the extremum of the second stop band increases, with increasing values for γ.

These results are comparable to those obtained in [5]. The present example will serve as a linear elastic reference case for the studies in Sect. 3 of this article, in which the interaction of viscoelastic behavior and imperfect bonding will be taken into account.

Comparison of the results from Sects. 2.1 and 2.2: In order to estimate the quality of the simulation of imperfect bonding by a thin interphase material $\Omega^{(2)}$ between the inclusion $\Omega^{(1)}$ and the matrix $\Omega^{(3)}$, we compare the frequency band structure for the approaches in Sect. 2.1, when imperfect bonding is simulated by the interphase $\Omega^{(2)}$, and in Sect. 2.2, when imperfect bonding is described by the boundary conditions in the interface $\partial\Omega_{1,3}$. Both approaches have been derived by application of the Floquet-Bloch theorem and the exact solution for the dispersion relation. One unit cell is again considered to have the length ℓ, and $r^{(1)}/\ell = 0.1$. The composite is composed of a polyethylene matrix ($G^{(3)} = 0.117$ GPa, $\rho^{(3)} = 910$ kg/m^3) and steel inclusions ($G^{(1)} = 80$ GPa, $\rho^{(1)} = 7860$ kg/m^3) [10].

- In the case of simulating the bonding condition between the inclusion $\Omega^{(1)}$ and the matrix $\Omega^{(3)}$ by an artificial interphase $\Omega^{(2)}$, as described in Sect. 2.1, we choose the properties $G^{(2)} = 10^{-3}$ GPa, $\rho^{(2)} = 1000$ kg/m^3, and $r^{(2)}/\ell = \left[r^{(1)} + \gamma G^{(2)}\right]/\ell$.
- In the case of imperfect bonding, which is described by the conjugate conditions at the interface $\partial\Omega_{1,3}$ between the inclusion and the matrix, we apply the interfacial conditions which have been derived in detail in Sect. 2.2.

The results are shown in Fig. 5 for different values of the bonding factor γ, with normalizations $\bar{\mu} = \mu\ell$ and $\bar{\omega} = \omega\ell$ applied. Both approaches to describe imperfect bonding coincide well, especially in the lower frequency region for the chosen values of the material parameters.

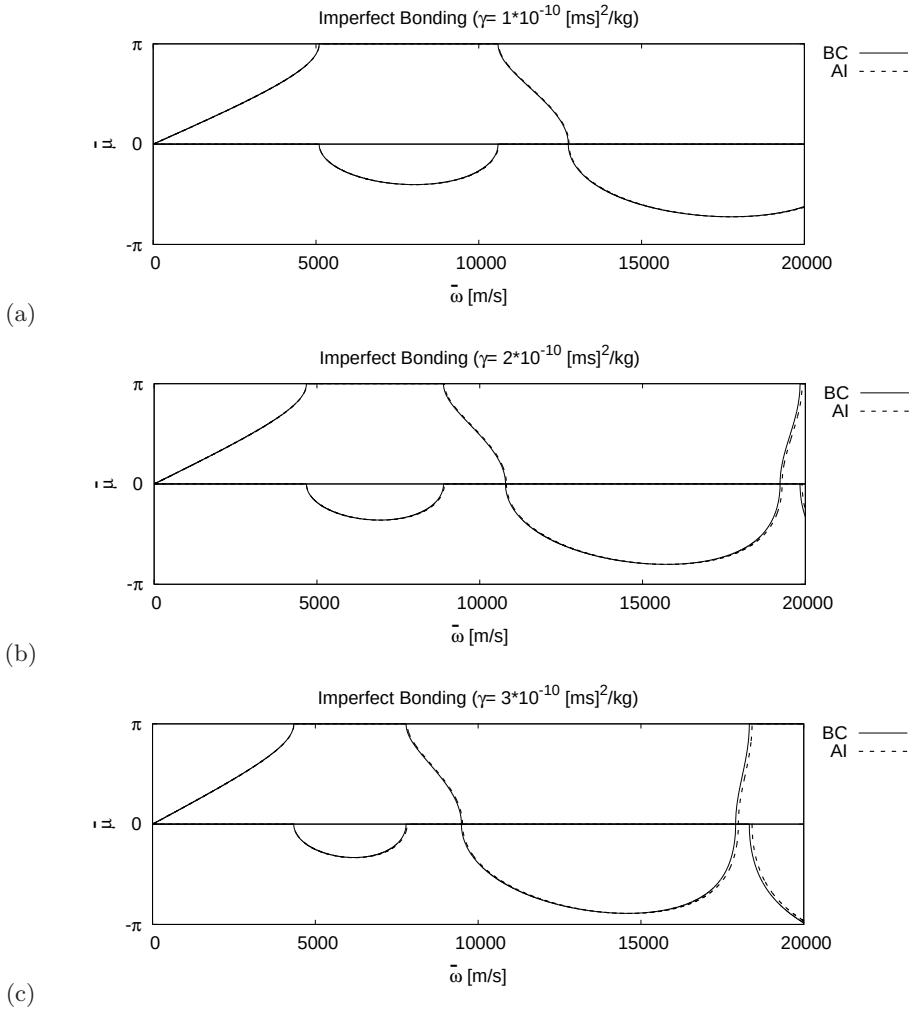

Fig. 5 Frequency band structure of a layered polyethylene ($G^{(3)} = 0.117$ GPa, $\rho^{(3)} = 910$ kg/m^3) and steel ($G^{(1)} = 80$ GPa, $\rho^{(1)} = 7860$ kg/m^3). In the case of bonding conditions described by the conjugate conditions at the interface $\partial\Omega_{1,3}$, different values for the bonding factor γ are chosen (BC). In the case of simulating the bonding condition between the inclusion and the matrix by an artificial interphase, we choose the properties $G^{(2)} = 10^{-3}$ GPa, $\rho^{(2)} = 1000$ kg/m^3, and $r^{(2)}/\ell = [r^{(1)} + \gamma G^{(2)}]\ell$. The pass bands ($\mu_R \neq 0, \mu_I = 0$) are plotted as positive values, and the stop bands ($\mu_R = 0, \mu_I \neq 0$) are plotted as negative values.

3 One-dimensional wave propagation in layered viscoelastic composites

In Sect. 2, the constituents have been taken to be linear elastic. Now we consider that the mechanical behavior of a matrix $\Omega^{(3)}$ depends on the frequency of the traveling signal. While in a purely elastic material the relation between stress and strain are in phase, e.g. both stress and strain appear simultaneously, in a viscoelastic material the phases of the stresses and the strains are shifted. The dynamic shear modulus $G^{(3)} = G^{(3)}(\omega)$ of the matrix is here now modeled as a Kelvin-Voigt type of material. Such a type of material is often represented by a spring, the elastic part of the mechanical behavior, which is parallel to a dashpot, may represent the viscous behavior of the material (also see Flügge [15]). The dynamic shear modulus is taken in the complex form

$$G^{(3)}(\omega) = G_R^{(3)} + jG_I^{(3)}(\omega), \tag{24}$$

where the real part $G_R^{(3)}$ is independent of the frequency, and $G_I^{(3)}(\omega)$ is the frequency-dependent imaginary part. We consider this imaginary part in the form

$$G_I^{(3)}(\omega) = \nu\, \omega\, G_R^{(3)}, \tag{25}$$

where ν is a constant with the dimension of time. This constant defines the imaginary part $G_I^{(3)}$ relative to the product of the frequency and the real part $G_R^{(3)}$. The product of ν and $G_R^{(3)}$ is also denoted as the viscosity. The viscosity of polymers depends on different factors, and for example, increasing temperature leads to an increased viscosity. If $\nu = 0$, then the material is purely elastic, and this case has been discussed in the Sects. 2.1 and 2.2. If $\nu \to \infty$, then the imaginary part of the dynamic shear modulus (25) would tend to $G_I^{(3)}(\omega) \to \pm\infty$ for $\omega \neq 0$.

The Kelvin-Voigt material has been chosen in order to model the viscoelastic behavior, because this relatively simple model allows us to quantify the viscous character of the solid by a single parameter ν, and therefore, it allows us to directly study the impact of the viscous part of the mechanical behavior on the frequency band structure. By taking into account further springs and dashpots with different mechanical properties in the mechanical modeling more accurate viscoelastic models can be developed [15].

In the following examples we want to illustrate the effect of viscoelastic behavior on the dispersion relation for layered two component composite described in Sect. 2.2, where the bonding between the constituents is taken to be imperfect, and the bonding condition between the constituents is quantified by the bonding factor γ which has been introduced in (21).

3.1 Numerical examples

We consider wave propagation though the layered composite shown in Fig. 2, where the constituents $\Omega^{(1)}$ is taken to be steel ($G^{(1)} = 80$ GPa, $\rho^{(1)} = 7860$ kg/m^3), and the constituents $\Omega^{(3)}$ is taken to be polyethylene with the dynamic modulus as given in (24). The real part is $G_R^{(3)} = 0.117$ GPa, $G_I^{(3)}(\omega)$ is given in (25), and $\rho^{(3)} = 910$ kg/m^3. The dispersion equation is obtained by solving the boundary value problem in (22) and (23). The numerical examples are subdivided into two parts. The first illustrates the dispersion relation for perfect bonding, and the second the interaction of imperfect bonding behavior.

Dispersion relation for perfect bonding: Figure 6 illustrates the results for perfect bonding ($\gamma = 0$) and different values for ν. The real values of the wave number μ_R are plotted as positive values,

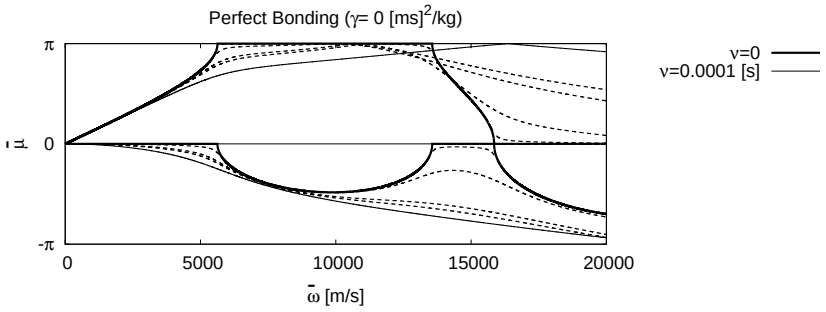

Fig. 6 Frequency band structure of a layered polyethylene ($G^{(3)}(\omega)$ in (24), where $G_R^{(3)} = 0.117$ GPa, and $G_I^{(3)}(\omega)$ is given in (25), $\rho^{(3)} = 910$ kg/m^3) and steel ($G^{(1)} = 80$ GPa, $\rho^{(1)} = 7860$ kg/m^3). Bonding between the constituents is taken to be perfect ($\gamma = 0$). The real values of the wave number μ_R are plotted as positive values, and the imaginary values of the wave number μ_I are plotted as negative values.

and the imaginary values of the wave number μ_I are plotted as negative values. The thick solid line

represents the elastic case ($\nu = 0$) as a reference. The thin solid line represents the case with the highest viscosity, $\nu = 10^{-4}$ s. The dashed lines show some intermediate values for ν ($\nu = 10^{-6}$ s, $\nu = 10^{-5}$ s, $\nu = 4 \cdot 10^{-5}$ s, $\nu = 5 \cdot 10^{-5}$ s) to depict the behavior of the dispersion relation with increasing viscosity.

In the elastic case, with $\nu = 0$, the boundaries between the pass bands and the stop bands are clearly defined by regions where either $\mu_R = 0$ or $\mu_I = 0$. With increasing viscosity, i.e., with increasing values for ν, the values for the attenuation factor μ_I increase and the gaps with $\mu_I = 0$ becomes narrower, and finally these gaps vanish.

These effects have been observed in different articles. Nemat-Nasser et al. [37] investigated one-dimensional wave propagation in a periodic steel-polymer composite, comparing the attenuation relation to experimental observations. Hussein et al. [24] discuss the dispersion relation for multiple layers in a one-dimensional unit cell with different arrangements with the goal to create a stop band with the maximum attenuation in a specific frequency region.

Dispersion relation for imperfect bonding: We consider the same material as in the previous paragraph, but now the bonding between $\Omega^{(1)}$ and $\Omega^{(3)}$ is taken to be imperfect and described by the bonding factor γ. The results are presented in Fig. 7. The influence of the bonding factor γ on the dispersion

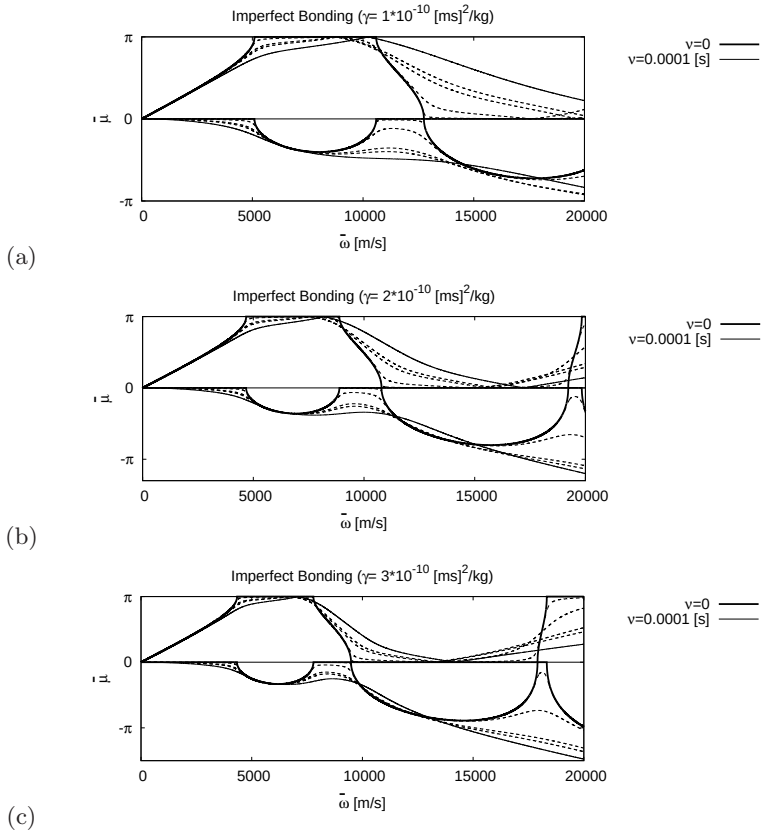

Fig. 7 Frequency band structure of a layered polyethylene ($G^{(3)}(\omega)$ in (24), where $G_R^{(3)} = 0.117$ GPa, and $G_I^{(3)}(\omega)$ is given in (25), $\rho^{(3)} = 910$ kg/m^3) and steel ($G^{(1)} = 80$ GPa, $\rho^{(1)} = 7860$ kg/m^3). Bonding between the constituents is taken to be imperfect and described by different values of the bonding factor γ. The real values of the wave number μ_R are plotted as positive values, and the imaginary values of the wave number μ_I are plotted as negative values.

relation for the elastic case has been discussed in in respect of the examples in Sect. 2.3. These cases of linear elastic behavior with $\nu = 0$ are represented by the thick solid lines as a reference. The thin solid line represents the case $\nu = 10^{-4}$ s, and the dashed lines show some intermediate values for ν ($\nu = 10^{-6}$ s, $\nu = 10^{-5}$ s, $\nu = 4 \cdot 10^{-5}$ s, $\nu = 5 \cdot 10^{-5}$ s) in (a)-(c). While for the here taken choices

for ν the curves for μ_I do not intersect within the presented frequency range for perfect bonding (see Fig. 6), in the case of imperfect bonding we find intersections of the μ_I-vs.-ω curves in all three panels of Fig. 7. For example, in (c) we can see for the frequency region around $\bar{\omega} = 11000$ m/s, that the attenuation μ_I decreases with increasing viscosity. Similar to the case of perfect bonding we find that with increasing values for ν the band gaps for μ_I becomes narrower and finally vanish.

This example shows the interaction of imperfect bonding and viscoelastic behavior. All curves shift to the left side with increasing values for γ, so that the attenuation of the traveling signal in general increases. This effect becomes obvious when we compare the attenuation factors μ_I at $\bar{\omega} = 20000$ in Fig. 7 (a), Fig. 7 (b), and Fig. 7 (c).

4 Plane-wave expansion method

The application of the Floquet-Bloch approach to obtain exact solutions for the dispersion relation is only possible for simple geometries. The plane-wave expansion method (PWEM) allows us to investigate wave propagation through periodic materials with more complex geometry. This approach is investigated in details in the present section. The PWEM is founded on the idea that a periodic function $s(x)$ with a period T can be represented as a Fourier series in the form

$$s(x) = \sum_{m=-\infty}^{\infty} c_m \exp(jm\omega x), \tag{26a}$$

$$c_m = \frac{1}{T}\int_0^T s(x)\exp(-jm\omega x)\,\mathrm{d}x. \tag{26b}$$

Taking into account a larger number of terms in (26) improves the accuracy of the solution. Although the PWEM is a useful methods, which allows us to investigate the frequency band structure of composites beyond the limitations of the Floquet-Bloch approach (see Sec. 2), it is crucial to be aware of the limitations of such method. This motivates us to subdivide the present section into two parts:

- In the first part we investigate the one-dimensional problem, which was presented in Sect. 2.1, and compare the results of the PWEM to the exact results. This has the goal to identify the limitations of the PWEM when applied to the analysis of the dispersion relations of composites.
- In the second part we apply this method to derive the dispersion relation for a composite with parallel fibers, in which a shear wave travels through the plane perpendicular to the fibers.

4.1 One-dimensional wave propagation in layered composites: PWEM versus exact solution

We consider the layered composite which has been presented in Fig. 1, which consists of the inclusion $\Omega^{(1)}$, the matrix $\Omega^{(3)}$, and the interphase $\Omega^{(2)}$. The wave equation for the traveling signal has been presented in Eq. (1). We consider a harmonic wave in the form

$$w(x,t) = F(x)\exp\left[j(\mu x + \omega t)\right], \tag{27}$$

which travels in x-direction through the material. The material parameters $G(x) = G(x+\ell)$ and $\rho(x) = \rho(x+\ell)$, and the function $F(x) = F(x+\ell)$ are periodic functions, and we want to represent these functions by their Fourier series in the form

$$F(x) = \sum_{m_1=-\infty}^{\infty} F_{m_1}\exp\left(j\frac{2\pi}{\ell}m_1 x_1\right), \tag{28a}$$

$$G(x) = \sum_{m_1=-\infty}^{\infty} G_{m_1}\exp\left(j\frac{2\pi}{\ell}m_1 x_1\right), \tag{28b}$$

$$\rho(x) = \sum_{m_1=-\infty}^{\infty} \rho_{m_1}\exp\left(j\frac{2\pi}{\ell}m_1 x_1\right), \tag{28c}$$

where G_{m_1} and ρ_{m_1} are determined via

$$G_{m_1} = \frac{1}{\ell}\int_0^\ell G(x)\exp\left(-j\frac{2\pi}{\ell}m_1 x_1\right)\,\mathrm{d}x_1, \tag{29a}$$

$$\rho_{m_1} = \frac{1}{\ell}\int_0^\ell \rho(x)\exp\left(-j\frac{2\pi}{\ell}m_1 x_1\right)\,\mathrm{d}x_1. \tag{29b}$$

If we substitute (28a) into (27), which then together with (28b) and (28c) is substituted into (1), then we obtain a wave equation in terms of an infinite number of terms, in the form

$$\sum_{m_1=-\infty}^{\infty} F_{m_1}\times\left\{G_{n_1-m_1}\left[\left(\frac{2\pi}{\ell}m_1+\mu_1\right)\left(\frac{2\pi}{\ell}n_1+\mu_1\right)\right]-\rho_{n_1-m_1}\omega^2\right\}=0. \tag{30}$$

To apply (30), we restrict the number terms to $|m_1| = |n_1| \leq m_{max}$.

The PWEM is an approach which approximates the solution of the dispersion relation. By taking into account a higher number of terms, e.g., by increasing m_{max}, the accuracy of the solution increases and higher frequencies are taken into consideration. On the other hand, by taking into account a higher number of terms the computation time increases, so that for efficient use of the plane-wave expansion method it is necessary to understand the limitations of this method, and quality of the results with every single term.

In order to estimate the limitations of the PWEM, we consider two examples, in which the results from the PWEM are compared to exact results.

Limitations of the plane-wave expansion method: We want to investigate the limitations of the PWEM by contrasting the solution for the dispersion relation obtained by the PWEM to the exact solution of the Floquet-Bloch method. Therefore, we consider the one-dimensional problem previously presented in Sect. 2.2, a layered composite with the inclusion $\Omega^{(1)}$, the matrix $\Omega^{(3)}$, and the interphase $\Omega^{(2)}$. The exact solution for the dispersion relation was provided by the solution of the boundary value problem in (22) and (23).

Figure 8 shows the frequency band structure of a layered composite with unit cell length ℓ. This composite consists of a polyethylene matrix ($G^{(3)} = 0.117$ GPa, $\rho^{(3)} = 910$ kg/m^3) and steel layers ($G^{(1)} = 80$ GPa, $\rho^{(1)} = 7860$ kg/m^3, $r^{(1)}/\ell = 0.1$). The interphase $\Omega^{(2)}$ has the properties $G^{(2)} = 10^{-3}$ GPa, $\rho^{(2)} = 1000$ kg/m^3, and $r^{(2)}\ell = [r^{(1)} + \gamma G^{(2)}]/\ell$. This Figure contrasts the exact results from the Floquet-Bloch approach (FB) with those obtained from the PWEM for $m_{max} = 0, 1, 2, 3, 4$.

- Fig. 8 (a) shows the results for the case of perfect bonding, $\gamma = 0$. With an increasing number of terms of the expansion, the solution of the PWEM approaches the exact solution. For the first branch of the dispersion relation the difference between the solution for $m_{max} = 4$ and the exact solution is relatively small, it becomes apparent that the differences for the second branch are relatively large.
- Fig. 8 (b) shows the results for imperfect bonding with the bonding factor $\gamma = 3 \cdot 10^{-10}$[ms]^2/kg. The differences in the results become even larger when imperfect bonding is taken into account. Note, that the results the PWEM in Figs. 8 (a) and 8 (b) are just slightly different.

These differences in the results are explained as follows: The ratio of the shear moduli $G^{(1)}/G^{(3)} = 683.8$ is relatively large in the present example, and $G(x)$ is a discontinuous function of $\mathbf{x}$. If a function is piece-wise defined, an overshoot appears at discontinuities. This overshoot reaches a limit, but it does not disappear with additional terms of the expansion. This effect is known as Gibbs phenomenon[1] [22]. In order to apply the plane-wave expansion method, the values for material parameters have to be relatively close together.

By comparing panels Figs. 8 (a) and 8 (b), we can conclude that imperfect bonding can only be taken into account by an interphase layer with material properties which describe slightly imperfect bonding.

[1] This phenomenon is also denoted as the Gibbs-Wilbraham phenomenon.

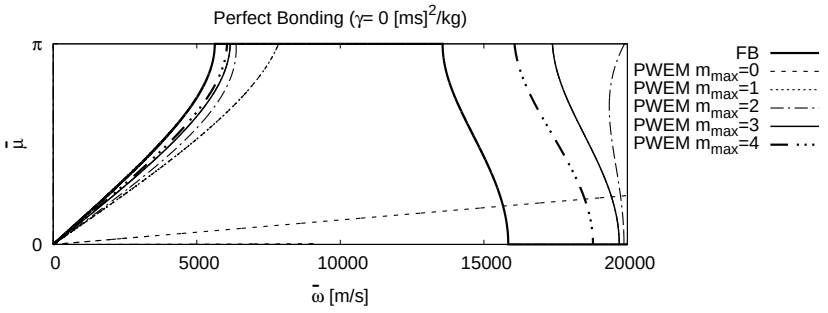

(a)

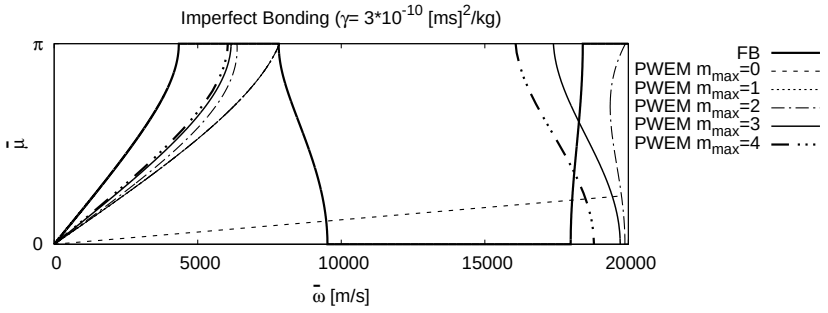

(b)

Fig. 8 Frequency band structure of a layered polyethylene ($G^{(3)} = 0.117$ GPa, $\rho^{(3)} = 910$ kg/m^3) and steel ($G^{(1)} = 80$ GPa, $\rho^{(1)} = 7860$ kg/m^3) composite. The exact results from the Floquet-Bloch approach (FB) with the results which are obtained from the PWEM for $m_{max} = 0, 1, 2, 3, 4$.

Wave propagation in a carbon-fiber matrix composite: The example in the previous paragraph discusses the limitations of the PWEM in the case of a high contrast between material parameters. In the present example, we choose a layered composite of unit cell with length ℓ, which consists of PANEX 33 carbon fibers ($G^{(1)} = 20$ GPa, $\rho^{(1)} = 1800$ kg/m^3, $r^{(1)}/\ell = 0.1$) which are embedded in EPON 828 polymer matrix (shear modulus $G^{(3)} = 1.287$ GPa, density $\rho^{(3)} = 1160$ kg/m^3). The material properties are taken from Wessel [47], Giurgiutiu et al. [18], and from the homepage of the company Hexion [1]. We choose an interphase $\Omega^{(2)}$ with mechanical properties (shear modulus $G^{(2)} = 5$ GPa, density $\rho^{(2)} = 1000$ kg/m^3, $r^{(2)}/\ell = 0.12$) which are of a similar order to the mechanical properties of the constituents $\Omega^{(1)}$ and $\Omega^{(3)}$. Figure 9 shows the dispersion relation for a layered composite. The results

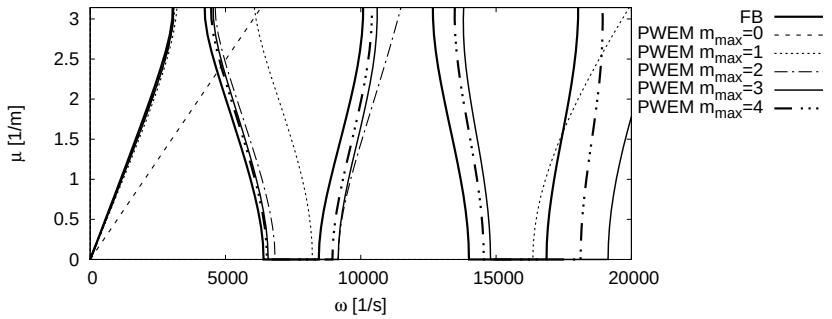

Fig. 9 Frequency band structure of a layered EPON 828 ($G^{(3)} = 1.287$ GPa, $\rho^{(3)} = 1160$ kg/m^3) and PANEX 33 ($G^{(1)} = 20$ GPa, $\rho^{(1)} = 1800$ kg/m^3, $r^{(1)}/\ell = 0.1$) composite with the interphase $\Omega^{(2)}$ ($G^{(2)} = 5$ GPa, $\rho^{(2)} = 1000$ kg/m^3, $r^{(2)}/\ell = 0.12$). The exact results from the Floquet-Bloch approach (FB) with the results which are obtained from the PWEM for $m_{max} = 0, 1, 2, 3, 4$.

obtained through use of the PWEM (30) for $m_{max} = 0, 1, 2, 3, 4$ are compared to results obtained by the boundary value problem in Eqs. (11) and (12). This Figure shows that for the first branch of the wave number, the results for $m_{max} \geq 1$ are relatively close to results for the exact solution. For the second branch of the wave number, the results for $m_{max} \geq 2$ approximate the exact solution. With higher frequencies, the differences between the exact results and the results of the PWEM become larger. On the other hand, these larger frequencies might exceed the range of realistic values for practical applications.

4.2 Two-dimensional wave propagation in a square lattice of inclusions

In this section we study the propagation of linear elastic anti-plane shear waves in a unidirectional fiber-reinforced composite, which is composed of the matrix $\Omega^{(3)}$ and parallel fibers $\Omega^{(1)}$. These fibers have a circular cross-section area and an infinite length occupying $-\infty \leq x_3 \leq \infty$. The fibers are coated by an interphase $\Omega^{(2)}$. One square unit cell of the composite has the side length ℓ, and the fiber is located in the center of each unit cell. The cross-sectional area of such a composite in the $\mathbf{E}_1 - \mathbf{E}_2$-plane is shown in Fig. 10. The basic translation vectors $\boldsymbol{\ell}$ then have the forms

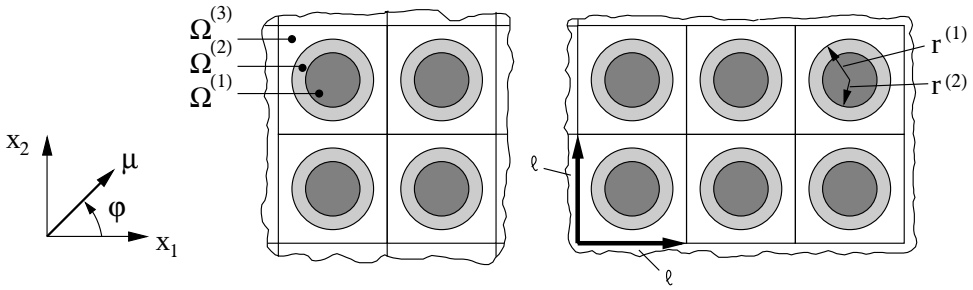

Fig. 10 The x_1-x_2 cross-section of a matrix-fiber composite.

$$\boldsymbol{\ell} = \mathbf{E}_1 r_1 \ell + \mathbf{E}_2 r_2 \ell, \tag{31}$$

where $\mathbf{E}_1$ and $\mathbf{E}_2$ are the base unit vectors of the Cartesian coordinate system, and r_1 and r_2 are the integers $0, \pm 1, \pm 2, \ldots$. A shear wave is assumed to propagate perpendicular to the fibers through the material in the x_1-x_2-plane, so that the wave equation can be presented in the form

$$\nabla_{\mathbf{x}} \left[G(\mathbf{x}) \nabla_{\mathbf{x}} w(\mathbf{x}, t) \right] = \rho(\mathbf{x}) \frac{\partial^2 w(\mathbf{x}, t)}{\partial t^2}, \tag{32}$$

where $\nabla_{\mathbf{x}} = \mathbf{E}_1 \frac{\partial}{\partial x_1} + \mathbf{E}_2 \frac{\partial}{\partial x_2}$, $G(\mathbf{x})$ and $\rho(\mathbf{x})$ are the shear modulus and the density, respectively, at the location $\mathbf{x} = \mathbf{E}_1 x_1 + \mathbf{E}_2 x_2$, and $w(\mathbf{x}, t)$ is the displacement in x_3-direction at the location $\mathbf{x}$ and time t. The traveling wave is taken in the form

$$w(\mathbf{x}, t) = F(\mathbf{x}) \exp\left(j \left[\boldsymbol{\mu} \cdot \mathbf{x} + \omega t \right] \right), \tag{33}$$

where $F(\mathbf{x}) = F(\mathbf{x} + p\boldsymbol{\ell})$ is a spatially periodic function, and $\boldsymbol{\mu} = \mathbf{E}_1 \mu_1 + \mathbf{E}_2 \mu_2$ is the wave vector. The length the wave vector $\mu = ||\boldsymbol{\mu}||$ is the wave number.

To derive the dispersion relation, the function $F(\mathbf{x})$ as well as the material properties $G(\mathbf{x})$ and $\rho(\mathbf{x})$ are now expanded into their Fourier series,

$$F(\mathbf{x}) = \sum_{m_1=-\infty}^{\infty} \sum_{m_2=-\infty}^{\infty} F_{m_1,m_2} \exp\left(j\frac{2\pi}{\ell}\left[m_1 x_1 + m_2 x_2\right]\right), \tag{34a}$$

$$G(\mathbf{x}) = \sum_{m_1=-\infty}^{\infty} \sum_{m_2=-\infty}^{\infty} G_{m_1,m_2} \exp\left(j\frac{2\pi}{\ell}\left[m_1 x_1 + m_2 x_2\right]\right), \tag{34b}$$

$$\rho(\mathbf{x}) = \sum_{m_1=-\infty}^{\infty} \sum_{m_2=-\infty}^{\infty} \rho_{m_1,m_2} \exp\left(j\frac{2\pi}{\ell}\left[m_1 x_1 + m_2 x_2\right]\right), \tag{34c}$$

where G_{m_1,m_2} and ρ_{m_1,m_2} are determined via

$$G_{m_1,m_2} = \frac{1}{\ell^2}\iint_{\Omega_0} G(\mathbf{x}) \exp\left(-j\frac{2\pi}{\ell}\left[m_1 x_1 + m_2 x_2\right]\right)\, \mathrm{d}x_1\, \mathrm{d}x_2, \tag{35a}$$

$$\rho_{m_1,m_2} = \frac{1}{\ell^2}\iint_{\Omega_0} \rho(\mathbf{x}) \exp\left(-j\frac{2\pi}{\ell}\left[m_1 x_1 + m_2 x_2\right]\right)\, \mathrm{d}x_1\, \mathrm{d}x_2. \tag{35b}$$

This specific form of the PWEM in (34) - (35) has also been derived in [3]. Let us substitute (34a) into (33), and then substitute this equation, together with the expansions of the material properties (34b) and (34c), into the wave equation (32). We then obtain the following system in the coefficients F_{m_1,m_2},

$$\begin{aligned}\sum_{m_1=-\infty}^{\infty} \sum_{m_2=-\infty}^{\infty} F_{m_1,m_2}\Bigg\{ G_{n_1-m_1,n_2-m_2}\Bigg[\left(\frac{2\pi}{\ell}m_1 + \mu_1\right)\left(\frac{2\pi}{\ell}n_1 + \mu_1\right) + \\ \left(\frac{2\pi}{\ell}m_2 + \mu_2\right)\left(\frac{2\pi}{\ell}n_2 + \mu_2\right)\Bigg] - \rho_{n_1-m_1,n_2-m_2}\omega^2\Bigg\} = 0.\end{aligned} \tag{36}$$

To apply (36) to determine the dispersion relation, we restrict the expansion in (36) to $|m_i| = |n_i| \leq m_{max}$, where $i = 1, 2$.

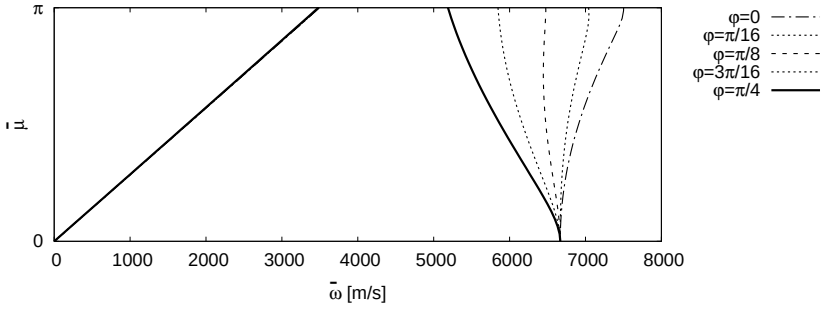

Fig. 11 Frequency band structure of EPON 828 matrix ($G^{(3)} = 1.287$ GPa, $\rho^{(3)} = 1160$ kg/m^3) and PANEX 33 fibers ($G^{(1)} = 20$ GPa, $\rho^{(1)} = 1800$ kg/m^3, $r^{(1)}/\ell = 0.1$) composite with the interphase $\Omega^{(2)}$ ($G^{(2)} = 5$ GPa, $\rho^{(2)} = 1000$ kg/m^3, $r^{(2)}/\ell = 0.12$). The results are obtained by the PWEM for $m_{max} = 1$ for different angles φ.

Shear wave propagation perpendicular to the fiber orientation: In this example we consider again a composite which consists of a EPON 828 polymer matrix (shear modulus $G^{(3)} = 1.287$ GPa, density $\rho^{(1)} = 1160$ kg/m^3, $r^{(1)}/\ell = 0.1$) and PANEX 33 carbon fibers ($G^{(1)} = 20$ GPa, $\rho^{(1)} = 1800$ kg/m^3, $r^{(1)}/\ell = 0.1$). We choose an interphase $\Omega^{(2)}$ with mechanical properties (shear modulus $G^{(2)} = 5$ GPa, density $\rho^{(2)} = 1000$ kg/m^3, $r^{(2)}/\ell = 0.12$) of the same order as the mechanical properties of the constituents $\Omega^{(1)}$ and $\Omega^{(3)}$.

The dispersion relation is shown in Fig. 11 for $m_{max} = 1$. The angle φ defines the direction of the propagating wave relative to the x_1-direction. For all angles φ the results for the first branch coincide. The second branch changes its shape as the values of φ, and the frequency range for the pass band vary.

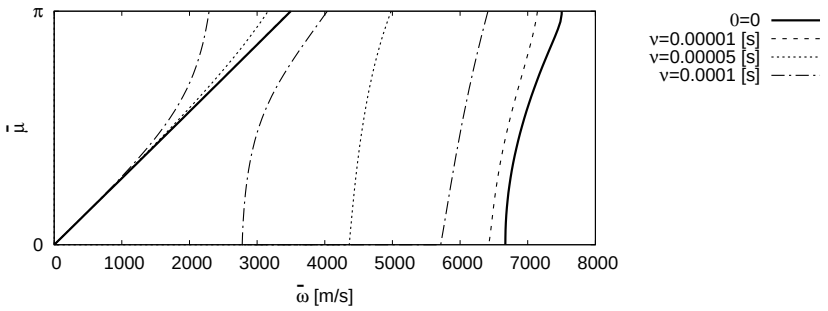

Fig. 12 Frequency band structure of a polymer matrix and PANEX 33 fibers ($G^{(1)} = 20$ GPa, $\rho^{(1)} = 1800$ kg/m^3, $r^{(1)}/\ell = 0.1$) composite with the interphase $\Omega^{(2)}$ ($G^{(2)} = 5$ GPa, $\rho^{(2)} = 1000$ kg/m^3, $r^{(2)}/\ell = 0.12$). Based on the properties of the material parameters of the EPON 828, the matrix is modeled as viscoelastic. The results are obtained by the PWEM for $m_{max} = 1$ and the propagation direction $\varphi = 0$ for different values of ν.

Let us now take the matrix to be viscoelastic, and the behavior of the matrix becomes frequency-dependent as given by (24). The real part of (24) is assumed to be given by $G_R^{(3)} = 1.287$ GPa, and the imaginary part is assumed to be described by (25). Figure 12 shows the dispersion relation which has been obtained by the PWEM for $m_{max} = 1$ and the propagation direction $\varphi = 0$ for different values of ν. This example illustrates the change of the shape and the location of the different branches of μ with increasing viscosity.

5 Discussion of the Results

This article deals with shear wave propagation through composites with periodic microstructures and the resulting dispersion relations. Sections 2 investigates coated inclusions and imperfect bonding between the constituents. To take imperfect bonding into account, two different approaches have been analyzed. In the first part, imperfect bonding has been simulated by an interphase material, and the properties of such an interphase describe the bonding conditions. This method is useful when bonding conditions cannot be explicitly described by the conjugate conditions at the interface between two constituents, for example when methods such as the plane-wave expansion method are applied. The disadvantage of this method is the fact that introducing a thin artificial layer to simulate the bonding conditions slightly changes the geometry of the considered problem, which has an impact on the dispersion relations, especially for higher frequencies. In the second case, bonding is described by the conjugate conditions at the common interface of the two constituents. Therefore, the spring-layer model has been applied, in which the difference of the displacements is proportional to the governing stresses in the interface. The difference in the displacements and the stresses are related by a proportionality constant γ, which is denoted as the bonding factor. Such a method is the preferred approach when the conjugate conditions can be explicitly taken into account, for example by the Floquet-Bloch method, as shown in this paper, or for other methods such as the asymptotic homogenization method, as for example discussed in [6, 13].

Although we restricted our considerations to a layered material, which consists of two components $\Omega^{(1)}$ and $\Omega^{(3)}$, and equal bonding conditions between these components at all interfaces, the herein presented results can be generalized for a layered material with an arbitrary number of components and with different bonding conditions. Studies for multiple-layer components and perfect bonding are well-known, for example from works such as Shen & Cao [41], and the herein presented results can be generalized analogously.

Different composites are composed of polymer constituents in which the material properties become frequency-dependent. Such material behavior has been in the focus of different studies on wave propagation [38, 24]. Section 3 has the goal to investigate the interaction between viscoelastic behavior and the bonding quality of the different constituents. It is shown that with decreasing bonding quality the attenuation of the wave decreases in composites with frequency-dependent material behavior.

Section 4 focuses on the application of the plane-wave expansion method to investigate the dispersion relation in composites. The first part analyzes the limitations of the method, and shows that, especially for a high contrast in the values of the material parameters, the results strongly deviate from the exact results due to the Gibbs phenomenon. A solution to this problem has been proposed in [4] by the application of Padé approximants. The second part of this section applies the plane-wave expansion method to investigate the dispersion relation for a fiber-reinforced composite, in which a shear wave propagates perpendicularly to the orientation of the parallel fibers. This example has been studies for different directions of the wave propagation, and for the case that one constituent shows frequency-dependent material behavior.

6 Conclusions

This article has shown that a combination of different approaches is useful to gain a deeper understanding of the properties of composites with periodic microstructures. The Floquet-Bloch approach allows us to obtain exact results for relatively simple geometries such as the layered composite, which have been discussed in the first part of our dispersion analysis. Although this method has limited practical value, it can still be considered to gain a basic understanding of the overall behavior of the composite. Methods to investigate more complex problems, such as the plane-wave expansion method, often approximate the results, and therefore it is necessary to understand the limitations of such methods. In our examples we have illustrated, that the application of the plane-wave expansion method is restricted to different factors, for example to composites with a relatively low contrast in the material parameters due to Gibbs phenomenon. The accuracy of the solutions by the plane-wave expansion method also depends on the number of terms, which are taken into account. On the other side a higher number of term requires an increased computation time.

Due to the limitations of the plane-wave expansion method, such an approach can be combined with further methods to understand the properties of composites. The need to combine different approaches in order to fully understand the mechanical behavior of composites has also been discussed in [2]. Within this paper, examples are based on material parameters, which may found in the literature, and on different assumptions and simplifications. Experiments might also be useful to justify the applied approaches.

A Dispersion relation for imperfect bonding between the constituents

From (22) and (23) we obtain a dispersion equation which gives the exact relation between the frequency ω, the wave number μ, and the bonding factor γ [44],

$$\begin{aligned}\cos(\mu\ell) = &\cos\left(2\mu^{(1)}r^{(1)}\right)\cos\left[\mu^{(1)}\left(\ell-2r^{(1)}\right)\right]\\ &-\frac{\left[z^{(1)}\right]^2+\left[z^{(2)}\right]^2}{2z^{(1)}z^{(2)}}\sin\left(2\mu^{(1)}r^{(1)}\right)\sin\left[\mu^{(1)}\left(\ell-2r^{(1)}\right)\right]\\ &-\gamma G^{(1)}\omega\left\{\sin\left(2\mu^{(1)}r^{(1)}\right)\cos\left[\mu^{(1)}\left(\ell-2r^{(1)}\right)\right]\right.\\ &\left.-\frac{z^{(2)}}{z^{(1)}}\cos\left(2\mu^{(1)}r^{(1)}\right)\sin\left[\mu^{(1)}\left(\ell-2r^{(1)}\right)\right]\right\}\\ &+\frac{1}{2}\frac{z^{(2)}}{z^{(1)}}\left(\gamma G^{(1)}\omega\right)^2\sin\left(2\mu^{(1)}r^{(1)}\right)\sin\left[\mu^{(1)}\left(\ell-2r^{(1)}\right)\right],\end{aligned} \tag{37}$$

where $z^{(i)}=\sqrt{G^{(i)}\rho^{(i)}}$.

In the limiting case of $\gamma=0$, the bonding between the matrix and the inclusions become perfect, and (37) reduces to

$$\begin{aligned}\cos(\mu\ell) = &\cos\left(2\mu^{(1)}r^{(1)}\right)\cos\left[\mu^{(1)}\left(\ell-2r^{(1)}\right)\right]\\ &-\frac{\left[z^{(1)}\right]^2+\left[z^{(2)}\right]^2}{2z^{(1)}z^{(2)}}\sin\left(2\mu^{(1)}r^{(1)}\right)\sin\left[\mu^{(1)}\left(\ell-2r^{(1)}\right)\right].\end{aligned} \tag{38}$$

Equation (38) is well-known for a two-components layered composite, and it can be found in different works such as Bedford & Drumheller [7].

Acknowledgements This work was supported by a Qatar University Internal Grant (QUUG-CAM-CAM-15/16-3) for H. Topol. This work has received funding from the European Union's Horizon 2020 research and innovation program under the Marie Sklodowska-Curie grant agreement no. 655177 for V.V. Danishevskyy.

References

1. Hexion homepage. https://www.hexion.com. Accessed: 21 April 2016
2. Andrianov, I.V., Awrejcewicz, J., Danishevs'kyy, V.V., Weichert, D.: Wave propagation in periodic composites: Higher-order asymptotic analysis versus plane-wave expansions method. J. Comput. Nonlinear Dynam. **6**, 011,015 (8 pages) (2011)
3. Andrianov, I.V., Bolshakov, V.I., Danishevs'kyy, V.V., Weichert, D.: Higher order asymptotic homogenization and wave propagation in periodic composite materials. Proc. R. Soc. A **464**, 1181–1201 (2008)
4. Andrianov, I.V., Danishevs'kyy, V.V., Ryzhkov, O.I., Weichert, D.: Numerical study of formation of solitary strain waves in a nonlinear elastic layered composite material. Wave Motion **51**, 405–417 (2014)
5. Andrianov, I.V., Danishevs'kyy, V.V., Topol, H.: Asymptotic homogenization for periodic composite materials with imperfect bonding conditions. In: V.I. Bolshakov, D. Weichert (eds.) Advanced Problems in Mechanics of Heterogeneous Media and Thin-Walled Structures. ENEM (2010)
6. Andrianov, I.V., Danishevs'kyy, V.V., Topol, H., Weichert, D.: Homogenization of a 1D nonlinear dynamical problem for periodic composites. Z. Angew. Math. Mech. **91**, 523–534 (2011)
7. Bedford, A., Drumheller, D.S.: Introduction to Elastic Wave Propagation. Wiley (1994)
8. Bloch, F.: Über die Quantenmechanik der Elektronen in Kristallgittern. Z. Phys. **52**, 555–600 (1928)
9. Brillouin, L.: Wave Propagation in Periodic Structures. Dover Publications (1953)
10. Crandall, S.H., Dahl, N.C., Lardner, T.J.: An Introduction to the Mechanics of Solids. McGraw-Hill (1959)
11. Craster, R.V., Joseph, L.M., Kaplunov, J.: Long-wave asymptotic theories: The connection between functionally graded waveguides and periodic media. Wave Motion **51**, 581–588 (2014)
12. Craster, R.V., Kaplunov, J., Nolde, E., Guenneau, S.: Bloch dispersion and high frequency homogenization for separable doubly-periodic structures. Wave Motion **49**, 333–346 (2012)
13. Danishevs'kyy, V.V., Kaplunov, J.D., Rogerson, G.A.: Anti-plane shear waves in a fibre-reinforced composite with a non-linear imperfect interface. Int. J. Nonlinear Mech. **76**, 223–232 (2015)
14. Floquet, G.: Sur les équations différentielles linéaires à coefficients périodiques. Ann. Sci. l'École Norm. Sup. **12**, 47–88 (1883)
15. Flügge, W.: Viscoelasticity. Springer (1975)
16. German, M., Pamin, J.: Modelling of corrosion interface in RC cross-section. In: R. Pęcherski, J. Rojek, P. Kowalczyk (eds.) Book of Abstracts of the 38th Solid Mechanics Conference, pp. 54–55. Institute of Fundamental Technological Research (IPPT). Polish Academy of Sciences (August 27-31, 2012)

17. Geymonat, G., Krasucki, F., Lenci, S.: Mathematical analysis of a bonded joint with a soft thin adhesive. Math. Mech. Solids **4**, 201–225 (1999)
18. Giurgiutiu, V., Reifsnider, K., Kriz, R., Ahn, B., Lesko, J.: Influence of fiber coating and interphase on the design of polymeric composite strength - analytical predictions. 36th Structures, Structural Dynamics and Materials Conference **36**, 453–469 (1995)
19. Goland, M., Reissner, E.: The stresses in cemented joints. J. Appl. Mech. **11**, 17–27 (1944)
20. Guz, A.N., Shul'ga, N.A.: Dynamics of laminated and fibrous composites. Appl. Mech. Rev. **45**, 35–60 (1992)
21. Hashin, Z.: Thin interphase/imperfect interface in elasticity with application to coated fiber composites. J. Mech. Phys. Solids **50**, 2509–2537 (2002)
22. Hewitt, E., Hewitt, R.E.: The Gibbs-Wilbraham phenomenon: An episode in Fourier analysis. Arch. Hist. Exact Sci. **21**, 129–160 (1979)
23. Hussein, M.I.: Theory of damped Bloch waves in elastic media. Phys. Rev. B **80**, 212 301 (2009)
24. Hussein, M.I., Hamza, K., Hulbert, G.M., Scott, R.A., Saitou, K.: Multiobjective evolutionary optimization of periodic layered materials for desired wave dispersion characteristics. Struct. Multidisc. Optim. **31**, 60–75 (2006)
25. Karpinos, D.M., Fedorenko, V.K.: Effect of protective coatings on the strength of the fiber-matrix bond in composite materials. Strength Mater. **8**, 445–448 (1976)
26. Klusemann, B., Svendsen, B.: Deviation of a model of adhesively bonded joints by the asymptotic expansion method. Int. J. Eng. Sci. **29**, 493–512 (1991)
27. Krasucki, F., Lenci, S.: Analysis of interfaces of variable stiffness. Int. J. Solids Struct. **37**, 3619–3632 (2000)
28. Kushwaha, M.S., Halevi, P., Martinez, G., Dobrzynski, L., Djafari-Rouhani, B.: Theory of acoustic band structure of periodic elastic composites. Phys. Rev. B **49**, 2313–2322 (1994)
29. Lebedev, L.P., Vorovich, I.I.: Functional Analysis in Mechanics. Springer (2003)
30. Lee, E.H., Yang, W.H.: On waves in composite materials with periodic structure. SIAM J. Appl. Math. **25**, 492–499 (1973)
31. Liu, Y., Yu, D., Zhao, H., Wen, J., Wen, X.: Theoretical study of two-dimensional phononic crystals with viscoelasticity based on fractional derivative models. Phys. Lett. A **41**, 065,503 (2008)
32. Lyapunov, A.M.: Stability of Motion. Academic Press (1966)
33. Mace, B.R., Manconi, E.: Wave motion and dispersion phenomena: Veering, locking and strong coupling effects. J. Acoust. Soc. Am. **131**, 1015–1028 (2012)
34. Mead, D.: Wave propagation in continuous periodic structures: research contributions from Southampton 1964-1995. J. Sound Vib. **190**, 495–524 (1996)
35. Merheb, B., Deymier, P.A., Jain, M., Aloshyna-Lesuffleur, M., Mohanty, S., Berker, A., Greger, R.W.: Elastic and viscoelastic effects in rubber/air acoustic band gap structures: A theoretical and experimental study. J. Appl. Phys. **104**, 064,913 (2008)
36. Movchan, A.B., Nicorovici, N.A., McPhedran, R.C.: Green's tensors and lattice sums for elastostatics and elastodynamics. Proc. R. Soc. A **453**, 643–662 (1997)
37. Nemat-Nasser, S., Sadeghi, H., Amirkhizi, A.V., Srivastava, A.: Phononic layered composites for stress-wave attenuation. Mech. Res. Commun. **68**, 65–69 (2015)
38. Nouh, M., Aldraihem, O., Baz, A.: Wave propagation in metamaterial plates with periodic local resonances. J. Sound Vib. **42**, 53–73 (2015)
39. Psarobas, I.E., Stefanou, N., Modinos, A.: Scattering of elastic waves by periodic arrays of spherical bodies. Phys. Rev. B **62**, 278–291 (2000)
40. Ruzzene, M., Baz, A.: Control of wave propagation in periodic composite rods using shape memory inserts. J. Vib. Acoust. **122**, 151–159 (2000)
41. Shen, M., Cao, W.: Acoustic bandgap formation in a periodic structure with multilayer unit cells. J. Phys. D: Appl. Phys. **33**, 1150–1154 (2000)
42. Shul'ga, N.A.: Theory of dynamic processes in mechanical systems and materials of regular structure. Int. Appl. Mech. **45**, 1301–1330 (2009)
43. Termonia, Y.: Fibre coating as a means to compensate for poor adhesion in fibre-reinforced materials. J. Mat. Sci. **25**, 103–106 (1990)
44. Topol, H.: Acoustic and mechanical properties of viscoelastic, linear elastic, and nonlinear elastic composites. Ph.D. thesis, RWTH Aachen University (2012)
45. Wang, W., Yua, J., Tang, Z.: General dispersion and dissipation relations in a one-dimensional viscoelastic lattice. Phys. Lett. A **373**, 5–8 (2008)
46. Wang, Y.F., Wang, Y.S., Laude, V.: Wave propagation in two-dimensional viscoelastic metamaterials. Phys. Lett. B **92**, 194,110–1–14 (2015)
47. Wessel, J.K.: The Handbook of Advanced Materials: Enabling New Designs. John Wiley & Sons (2004)